



Structural relations and pseudosymmetries in the andorite homologous series

Massimo Nespolo, Tohru Ozawa, Yusuke Kawasaki, Kazumasa Sugiyama

► To cite this version:

Massimo Nespolo, Tohru Ozawa, Yusuke Kawasaki, Kazumasa Sugiyama. Structural relations and pseudosymmetries in the andorite homologous series. *Journal of mineralogical and petrological sciences*, 2012, 107 (6), pp.226 - 243. 10.2465/jmps.120730 . hal-01711518

HAL Id: hal-01711518

<https://hal.univ-lorraine.fr/hal-01711518>

Submitted on 21 Feb 2018

HAL is a multi-disciplinary open access archive for the deposit and dissemination of scientific research documents, whether they are published or not. The documents may come from teaching and research institutions in France or abroad, or from public or private research centers.

L'archive ouverte pluridisciplinaire **HAL**, est destinée au dépôt et à la diffusion de documents scientifiques de niveau recherche, publiés ou non, émanant des établissements d'enseignement et de recherche français ou étrangers, des laboratoires publics ou privés.

Structural relations and pseudosymmetries in the andorite homologous series

Massimo NESPOLO*, Tohru OZAWA**, Yusuke KAWASAKI** and Kazumasa SUGIYAMA***

*Université de Lorraine, Faculté des Sciences et Technologies, Institut Jean Barriol FR 2843, CRM2 UMR CNRS 7036. BP 70239,

Boulevard des Aiguillettes F54506 Vandoeuvre-lès-Nancy cedex, France

**Department of Earth and Planetary Science, The University of Tokyo, 7-3-1 Hongo, Bunkyo-Ku, 113-0033 Tokyo, Japan

***Institute for Material Research, Tohoku University, 2-1-1 Katahira, Aoba-ku, Sendai 980-8577, Japan

The structure of quatranderite is reported for the first time from an untwinned sample from Oura mine, San Jose, Bolivia. The mineral crystallizes in $P2_1/c$, $a = 19.1686$ (19) Å, $b = 17.160$ (3) Å, $c = 13.042$ (2) Å, $\beta = 90.008$ (12)°, $V = 4289.9$ (11) Å³, $Z = 4$. Refinement to $R_{\text{obs}} = 5.66\%$ was obtained with Jana2006. Quatranderite belongs to the andorite series, whose members share two cell parameters while the third can be expressed as $n \times 4.3$ Å, with $n = 2, 4$ and 6 for ramdohrite (uchucchacuaite, fizelyite), quatranderite and senanderite, respectively. Both quatranderite and senanderite are strongly pseudosymmetric up to $Cmcm$ with one parameter corresponding to $n = 1$ (~ 4.3 Å). The hypothetical structure corresponding to $Cmcm$ is also the aristotype common to both minerals. The strong structural similarity of quatranderite and senanderite may explain their co-existence in some samples, which has in the past led to hypothesize the existence of a further member of the series, nakaséite, which was however later shown to consist of a random stacking of the two minerals. The $Cmcm$ aristotype is not common to the $n = 2$ minerals (uchucchacuaite, ramdohrite, fizelyite), which are thus structurally less closely related to the two other members. A common aristotype to all three minerals can nevertheless be obtained via a different path, which leads to $Cmme$ with the same cell parameters as $Cmcm$; the degree of pseudo-symmetry in this supergroup is however lower and there remain a difference in one sulfur position in this aristotype. It nevertheless confirms previous reports in the literature stating that the bulk of the structure of the minerals of this series can be reduced to a common principle, essentially a distorted galena; the departures from it are however crucial for the realization of the individual structures.

Keywords: Andorite, Crystal structure, Pseudo-symmetry, Homologous series, Modularity

INTRODUCTION

The andorite series of sulfosalts includes orthorhombic and pseudo-orthorhombic monoclinic minerals whose ideal chemical compositions can be expressed as $n(\text{PbAgMn})_{2+x}\text{Sb}_{3-x}\text{S}_6$ with approximate cell parameters $a = 19$, $b = 13$, and $c = n \times 4.3$ Å, apart from axes permutations to achieve a standard setting of the space group, and a slight deviation from the orthorhombic metric in the monoclinic minerals. Members of this series include ramdohrite ($x = 0.25$, $n = 2$), fizelyite ($x = 0.375$, $n = 2$), uchucchacuaite ($x = 0.5$, $n = 2$), quatranderite ($x = 0$, $n = 4$,

previously reported as andorite-IV) and senanderite ($x = 0$, $n = 6$, previously reported as andorite-VI). Ito and Muraoka (1960) described another member of this series having $n = 24$ for which they proposed the name nakaséite; this has, however, been shown to consist of a random stacking of $n = 4$ and $n = 6$ slabs giving an apparent period $n = 24$ (Moëlo et al., 1989).

The crystal structures of ramdohrite (Makovicky and Mumme, 1983), Ag-rich fizelyite (Yang et al. 2009), uchucchacuaite (Yang et al., 2011), and senanderite (Sawada et al. 1987) have been reported in the literature. New data about the ramdohrite structure from the same sample have been obtained but are still unpublished (Makovicky, personal communication to MN). A search in the ICSD database (Belsky et al., 2002) did not reveal other

doi:10.2465/jmps.120730

M. Nespolo, Massimo.Nespolo@crm2.uhp-nancy.fr Corresponding author

structure reports; in particular, no structure of quatrandorite has been found, which was reported to be systematically twinned (Moëlo et al., 1989). We report here the crystal structure of untwinned quatrandorite and investigate the structural relations in this series up to their aristo-types via a search for pseudo-symmetries and the corresponding modified Bärnighausen (1980) trees.

EXPERIMENTAL

The sample of quatrandorite was obtained from Oura mine, San Jose, Bolivia. The chemical composition was determined by EPMA (Electron Probe Micro Analysis). The result, corresponding to $\text{Pb}_{4.2}\text{Cu}_{0.2}\text{Ag}_{3.6}\text{Fe}_{0.1}\text{Sb}_{11.5}\text{As}_{0.4}\text{S}_{24}$, was obtained by averaging the results at several points. In the following, the composition is approximated to $4[\text{PbAgSb}_3\text{S}_6]$, the minor components having no practical effect on the refinement results.

A crystal was cut from the above sample to nearly cubic shape, with size $0.08 \times 0.09 \times 0.10 \text{ mm}^3$ and mounted on a Rigaku AFC-7R four-circle X-ray diffractometer equipped with a rotating anode. Experimental details are given in Table 1. Cell parameters have been refined from 25 reflections with final values $a = 19.1686(19) \text{ \AA}$, $b = 17.160(3) \text{ \AA}$, $c = 13.042(2) \text{ \AA}$, $\beta = 90.008(12)^\circ$. Intensities are compatible with a space group of type $P2_1/c$ (No. 14).

Structure solution was performed by charge flipping with the Superflip program included in Jana2006 (Petricek et al., 2006). Refinement was performed with Jana2006 on 9857 reflections, of which 6173 having $I/\sigma(I) > 3$ considered as ‘‘observed reflections’’. The absorption correction was performed by the common Ψ -scan procedure (North et al., 1968). The model obtained from Superflip was at first refined with isotropic thermal displacement parameters, leading to $R_{\text{obs}} = 8.60\%$ ($wR_{\text{obs}} = 9.09\%$) for

177 parameters. Anisotropic thermal displacement was then introduced, and the refinement converged smoothly to $R_{\text{obs}} = 5.66\%$ ($wR_{\text{obs}} = 6.28\%$; details in Table 1) for 397 parameters, with a largely comfortable ratio reflections/parameters 24.8 (15.5 for observed). To explore the possibility of isomorphic replacement in the cation sites, we performed an additional refinement by placing lead in all the sites and refining the occupancy. The results were consistent with the occupancies in the previous model and did not suggest any significant substitution.

Despite the systematic twinning reported by Moëlo et al. (1989), our sample did not show any evidence of twinning. The lattice being practically orthorhombic within the standard uncertainty and the structure being monoclinic holohedral, twinning would correspond to metric merohedry, or Class IIB (Nespolo and Ferraris, 2000), i.e., the twin operation would belong to the symmetry of the lattice and correspond to a higher crystal family (orthorhombic). No splitting of reflections would appear even at high angles. Furthermore, being a Class IIB twinning, the structure refinement would not converge even for equivalent individuals unless twinning is taken into account in the refinement strategy. Under these conditions, the quality of the refinement is a definite proof of the absence of twinning in the sample.

Details of the refinement results are given in Table 1. Fractional atomic coordinates and isotropic thermal displacement parameters are shown in Table 2. Table 3 gives the anisotropic thermal displacement parameters. Selected bond distances are in Table 4. The CIF (Crystallographic Information File) and the list of reflections are available as supplementary material from the publisher.

MODULARITY IN THE ANDORITE SERIES

Homologous series are modular structures, i.e., structures built by periodically juxtaposing one (‘monoarchetypal structures’) or more (‘polyarchetypal structures’) type of modules. Monoarchetypal structures are cell-twins, namely structures built by the polysynthetic repetition of a module according to an operation which is geometrically reminiscent of a twin operation but operates at the unit-cell level.

The simplest case of modular structure is that of polytypes: one crystal-chemically well defined module (usually a layer) is repeated according to a cell-twin operation which produces different orientations and/or displacements, giving rise to a stacking ambiguity. With a few exceptions, which also depend on the degree of idealization in the description of the layers, layer pairs are geometrically equivalent and polytypes fit the criteria of OD structures (Dornberger-Schiff, 1956). Because the cell-

Table 1. Experimental details

Crystal data	Data collection
$\text{Ag}_4\text{Pb}_4\text{Sb}_{12}\text{S}_{24}$	Rigaku AFC-7R
$M_r = 3490.7$	Absorption correction: psi-scan
$D_x = 5.403$	10293 measured reflections
Monoclinic, $P2_1/c$	9857 independent reflections
$a = 19.1686(19) \text{ \AA}$	6173 reflections with $I > 3(I)$
$b = 17.160(3) \text{ \AA}$	$R_{\text{int}}(\text{obs}) = 4.04$
$c = 13.042(2) \text{ \AA}$	$R_{\text{int}}(\text{all}) = 4.70$
$\beta = 90.008(12)^\circ$	Refinement
$V = 4289.9(11) \text{ \AA}^3$	$R[F^2 > 3(F^2)] = 0.0566$
$Z = 4$	$wR[F^2 > 3(F^2)] = 0.0628$
Mo $K\alpha$ radiation	$S(\text{GooF}) = 1.72$
$\mu = 26 \text{ mm}^{-1}$	6173 reflections
$T = 293 \text{ K}$	397 parameters
$0.08 \times 0.09 \times 0.10 \text{ mm}$	$\text{Max} = 2.93 \text{ e \AA}^{-3}$
	$\text{Min} = -5.21 \text{ e \AA}^{-3}$

Table 2. Quatrandorite fractional atomic coordinates and isotropic thermal displacement factors

Atom	<i>x</i>	<i>y</i>	<i>z</i>	<i>U</i> _{iso}	Atom	<i>x</i>	<i>y</i>	<i>z</i>	<i>U</i> _{iso}
Pb1	0.24276(4)	0.82487(4)	0.57335(6)	0.0237(2)	S1	0.3995(2)	0.7024(2)	0.0244(4)	0.0209(13)
Pb2	0.25023(4)	0.30831(5)	0.60330(7)	0.0320(3)	S2	0.0159(2)	0.1999(2)	0.2932(3)	0.0173(12)
Pb3	0.25544(4)	0.06872(5)	0.58827(6)	0.0282(2)	S3	0.1061(2)	0.1692(2)	0.0071(3)	0.0175(12)
Pb4	0.24888(4)	0.93783(5)	0.08883(7)	0.0324(3)	S4	0.1548(2)	0.7929(2)	0.2177(3)	0.0178(13)
Sb1	0.12058(6)	0.68987(6)	0.34641(9)	0.0163(3)	S5	0.0940(2)	0.6488(2)	0.9912(3)	0.0188(13)
Sb2	0.95572(6)	0.30075(6)	0.38704(9)	0.0168(3)	S6	0.4958(2)	0.8360(2)	0.7653(4)	0.0228(14)
Sb3	0.44664(6)	0.81586(6)	0.12447(9)	0.0164(3)	S7	0.1713(2)	0.3129(3)	0.2192(4)	0.0215(13)
Sb4	0.44792(6)	0.18462(7)	0.62519(9)	0.0168(3)	S8	0.2336(2)	0.6901(3)	0.4355(3)	0.0225(14)
Sb5	0.05798(6)	0.32777(6)	0.13344(9)	0.0151(3)	S9	0.4083(2)	0.2882(2)	0.5053(4)	0.0215(14)
Sb6	0.36327(6)	0.19028(6)	0.37208(9)	0.0175(3)	S10	0.3415(2)	0.1853(3)	0.7276(4)	0.0216(13)
Sb7	0.14971(6)	0.06736(6)	0.87612(9)	0.0181(3)	S11	0.2441(2)	0.1953(3)	0.4507(4)	0.0216(13)
Sb8	0.06031(6)	0.06498(7)	0.12385(9)	0.0161(3)	S12	0.3405(2)	0.8225(3)	0.2387(3)	0.0212(13)
Sb9	0.37354(6)	0.93441(7)	0.35266(9)	0.0179(3)	S13	0.0973(2)	0.9624(2)	0.0033(3)	0.0174(13)
Sb10	0.44131(6)	0.92230(7)	0.63262(10)	0.0205(4)	S14	0.0031(2)	0.4087(2)	0.2728(4)	0.0185(13)
Sb11	0.04508(6)	0.56303(6)	0.11976(9)	0.0161(3)	S15	0.3440(2)	0.0403(3)	0.2272(4)	0.0202(13)
Sb12	0.54567(7)	0.94662(7)	0.88204(10)	0.0221(4)	S16	0.0977(2)	0.4419(2)	0.0280(3)	0.0175(13)
Ag1	0.35709(8)	0.81311(9)	0.84948(12)	0.0308(5)	S17	0.1527(2)	0.5768(2)	0.2330(3)	0.0168(13)
Ag2	0.14280(10)	0.17732(12)	0.33615(18)	0.0618(8)	S18	0.4824(3)	0.0421(3)	0.7810(4)	0.0257(15)
Ag3	0.35640(11)	0.05251(12)	0.82640(17)	0.0563(7)	S19	0.2582(2)	0.9446(2)	0.4278(3)	0.0191(13)
Ag4	0.13216(11)	0.93297(11)	0.33294(15)	0.0484(6)	S20	0.4010(3)	0.9114(3)	0.0031(4)	0.0231(14)
					S21	0.4033(2)	0.0815(2)	0.5084(4)	0.0207(14)
					S22	0.1637(2)	0.0536(2)	0.2278(3)	0.0186(13)
					S23	0.2679(3)	0.0633(3)	0.9577(4)	0.0267(15)
					S24	0.3285(2)	0.9297(3)	0.7144(4)	0.0213(14)

In parenthesis the standard uncertainty.

twin operation leading to polytypism does not alter the chemistry, polytypes have by definition the same composition as the layer¹⁾. When instead the cell-twin operation is accompanied by the creation or annihilation of atomic positions at the boundary of a module, this results in *chemical twins*: the term comes from the fact that the chemistry can be modified by that cell-twin operation. When this mechanism operates to create a series of structures varying both in the structure and in the chemistry because of the variable width of the module building the different members of the series, the phenomenon is called tropochemical cell-twinning (Takéuchi, 1997; for a recent review, see Nespolo et al., 2004).

Tropochemical cell-twinning is particularly active in sulfides, as shown by the lillianite series, where the different members of the series are characterized by a variable width of the PbS module (Takéuchi, 1997). The andorite series, however, differs fundamentally from the lillianite series because its members keep the same width of the module but differ for the stacking of this module along the perpendicular direction, to form what Moëlo et al. (1989) have called 'floors' ('étages') rather than layers.

This is clearly shown in Figures 1 to 3, where the structures of uchucchacuaite, quatrandorite and senandorite are shown in projection along the axis of variable period (*c* axis for uchucchacuaite and *b* axis for the two other members), with the axis having a period about 19 Å taken horizontal (*a* for uchucchacuaite and quatrandorite, *c* for senandorite). Apart from slight deformations and the presence of cation substitutions, the module thickness is about half of the horizontal period (19 Å) (drawings of structures have been obtained with the software VESTA: Momma and Izumi, 2008). This module is cell-twinned on (100) in uchucchacuaite and quatrandorite, and on (001) in senandorite. Another projection, along the axis corresponding to about 13 Å, always with the axis corresponding to about 19 Å horizontal, is shown in Figures 4–6 from which no further insight can be easily obtained. For a better understanding of the structural relationships in this series, we performed a search for aristotypes.

SEARCH FOR A COMMON ARISTOTYPE

An aristotype (Megaw, 1973), or basic structure (Buerger, 1947), is a real or fictitious high-symmetry structure from which lower-symmetry structures (known as hettotypes or derivative structures) can be obtained by reducing the point and/or translational symmetry. Hettotypes are clas-

¹⁾ The fact that in practice some tolerance is accepted when fitting related structures into the definition of polytypes does not alter the classification scheme.

Table 3. Quatrandorite anisotropic thermal displacement factors

Atom	U11	U22	U33	U12	U13	U23
Pb1	0.0287(4)	0.0199(4)	0.0225(4)	-0.0009(3)	0.0049(3)	0.0008(3)
Pb2	0.0301(5)	0.0318(4)	0.0341(5)	-0.0072(4)	-0.0008(4)	-0.0010(4)
Pb3	0.0290(4)	0.0265(4)	0.0291(4)	-0.0009(3)	0.0003(3)	0.0024(3)
Pb4	0.0359(5)	0.0293(4)	0.0319(5)	-0.0091(4)	-0.0043(4)	0.0065(3)
Sb1	0.0198(6)	0.0159(5)	0.0133(6)	0.0006(5)	0.0018(5)	-0.0001(5)
Sb2	0.0175(6)	0.0152(5)	0.0176(6)	0.0011(5)	0.0051(5)	-0.0021(5)
Sb3	0.0150(6)	0.0151(5)	0.0191(6)	0.0015(5)	0.0002(5)	-0.0012(5)
Sb4	0.0120(6)	0.0184(5)	0.0200(6)	0.0003(5)	0.0001(5)	0.0009(5)
Sb5	0.0143(6)	0.0133(5)	0.0177(6)	0.0011(4)	0.0038(5)	-0.0014(4)
Sb6	0.0176(6)	0.0149(5)	0.0200(6)	0.0015(5)	-0.0016(5)	-0.0015(5)
Sb7	0.0210(6)	0.0136(5)	0.0198(6)	-0.0001(5)	0.0044(5)	-0.0005(5)
Sb8	0.0144(6)	0.0172(5)	0.0168(6)	0.0002(5)	0.0025(5)	-0.0023(5)
Sb9	0.0166(6)	0.0213(6)	0.0157(6)	0.0004(5)	0.0021(5)	-0.0012(5)
Sb10	0.0158(6)	0.0243(6)	0.0213(7)	0.0037(5)	0.0032(5)	0.0049(5)
Sb11	0.0169(6)	0.0148(5)	0.0167(6)	-0.0022(5)	0.0021(5)	0.0002(5)
Sb12	0.0209(7)	0.0222(6)	0.0231(7)	0.0060(5)	0.0009(5)	0.0031(5)
Ag1	0.0322(9)	0.0287(8)	0.0313(9)	-0.0072(7)	0.0087(7)	0.0000(7)
Ag2	0.0378(11)	0.0693(14)	0.0782(16)	0.0158(10)	-0.0330(11)	-0.0359(12)
Ag3	0.0474(12)	0.0566(12)	0.0647(14)	0.0084(10)	0.0329(11)	-0.0015(10)
Ag4	0.0552(12)	0.0498(11)	0.0401(11)	-0.0224(9)	-0.0096(9)	0.0213(9)
S1	0.023(2)	0.018(2)	0.022(2)	-0.0041(18)	0.000(2)	-0.0057(18)
S2	0.016(2)	0.015(2)	0.021(2)	0.0001(17)	0.0036(18)	-0.0021(17)
S3	0.020(2)	0.0131(19)	0.020(2)	0.0022(17)	0.0008(18)	0.0014(16)
S4	0.014(2)	0.018(2)	0.022(2)	-0.0022(16)	0.0026(18)	-0.0020(17)
S5	0.019(2)	0.016(2)	0.022(2)	-0.0008(17)	0.0025(19)	0.0044(17)
S6	0.024(3)	0.012(2)	0.033(3)	0.0018(17)	-0.011(2)	-0.0020(18)
S7	0.013(2)	0.023(2)	0.028(3)	0.0019(18)	0.0024(19)	0.0022(19)
S8	0.025(2)	0.023(2)	0.020(2)	0.001(2)	-0.0034(19)	-0.0047(19)
S9	0.019(2)	0.015(2)	0.030(3)	-0.0007(17)	-0.001(2)	0.0047(18)
S10	0.018(2)	0.024(2)	0.023(2)	0.0013(19)	0.0013(19)	-0.0002(19)
S11	0.019(2)	0.021(2)	0.024(2)	-0.0007(19)	-0.0006(19)	0.0021(19)
S12	0.023(2)	0.024(2)	0.017(2)	-0.0050(19)	0.0060(19)	-0.0062(18)
S13	0.016(2)	0.0146(19)	0.021(2)	-0.0025(17)	0.0017(19)	-0.0040(17)
S14	0.021(2)	0.0106(19)	0.024(2)	-0.0011(17)	0.0093(19)	0.0003(17)
S15	0.019(2)	0.022(2)	0.020(2)	-0.0001(18)	-0.0013(19)	0.0021(18)
S16	0.021(2)	0.0134(19)	0.018(2)	0.0015(17)	0.0056(18)	0.0007(17)
S17	0.017(2)	0.021(2)	0.012(2)	-0.0022(17)	-0.0012(17)	-0.0018(17)
S18	0.021(2)	0.016(2)	0.039(3)	0.0019(18)	-0.005(2)	0.005(2)
S19	0.017(2)	0.022(2)	0.019(2)	0.0016(18)	0.0057(18)	0.0027(18)
S20	0.028(3)	0.020(2)	0.021(2)	0.0023(19)	0.000(2)	0.0036(19)
S21	0.019(2)	0.017(2)	0.026(3)	0.0011(18)	0.000(2)	-0.0042(18)
S22	0.015(2)	0.020(2)	0.021(2)	0.0026(17)	0.0003(18)	0.0008(18)
S23	0.022(2)	0.020(2)	0.038(3)	-0.002(2)	0.010(2)	-0.001(2)
S24	0.017(2)	0.025(2)	0.023(2)	0.0010(19)	-0.0004(19)	-0.0035(19)

In parenthesis the standard uncertainty.

sified in substitution structures and distortion structures. The latter correspond to displacive phase transitions, where the aristotype (parent phase) and the hettotype (daughter phase) are in group-subgroup relation, like for example in the case of the beta-quartz to alpha-quartz transition. Substitution structures, instead, are obtained when two or more different kinds of atoms replace one kind of atom in the aristotype and consequently the space-group symmetry decreases. Some atomic sites that were

equivalent in the aristotype may be divided into two or more different sites in the hettotype, a phenomenon known as splitting of Wyckoff positions (Wondratschek, 1993). A typical simple example is the structure of sphalerite as the hettotype of the structure of diamond, where carbon atoms are alternatively replaced by zinc and sulfur.

The search for an aristotype takes a special meaning in case of modular structures. For OD structures, the ultimate aristotype corresponds to the so-called family struc-

Table 4. Interatomic cation-sulphur distances in quatrandorite

Pb1	S1	3.106(5)	Sb1	S4	2.525(4)	Sb10	S1	2.686(5)
	S4	3.236(4)		S8	2.458(5)		S6	2.505(5)
	S5	3.079(5)		S17	2.516(4)		S24	2.415(5)
	S8	2.934(5)	Sb2	S2	2.414(4)	Sb11	S2	2.859(4)
	S17	3.188(4)		S4	2.523(5)		S5	2.421(5)
	S19	2.813(4)		S14	2.545(5)		S16	2.603(4)
Pb2	S24	3.053(5)	Sb3	S1	2.512(5)	Sb12	S17	2.548(4)
	S3	3.058(5)		S12	2.525(5)		S6	2.614(5)
	S7	2.984(5)		S20	2.441(5)		S15	2.560(5)
	S10	3.184(5)	Sb4	S9	2.487(5)	Ag1	S18	2.427(5)
	S11	2.782(5)		S10	2.439(5)		S6	2.903(5)
	S23	2.928(5)		S21	2.487(5)		S8	2.620(5)
Pb3	S7	3.106(5)	Sb5	S7	2.456(5)	Ag2	S12	2.758(5)
	S10	3.166(5)		S14	2.518(5)		S20	2.751(5)
	S11	2.825(5)		S16	2.511(4)		S24	2.722(5)
	S16	3.129(5)	Sb6	S9	2.567(5)	Ag3	S2	2.526(5)
	S19	2.987(5)		S10	2.878(5)		S7	2.835(5)
	S21	3.029(5)		S11	2.505(5)		S11	2.470(5)
Pb4	S24	3.218(5)	Sb7	S21	2.690(5)	Ag4	S22	2.581(5)
	S8	2.984(5)		S3	2.583(4)		S10	2.634(5)
	S12	3.289(5)		S7	2.929(5)		S18	2.494(5)
	S13	3.140(4)	Sb8	S13	2.646(4)	Ag4	S23	2.418(6)
	S15	3.110(5)		S23	2.504(5)		S24	2.619(5)
	S20	3.155(5)		S3	2.508(4)		S4	2.868(5)
	S22	3.147(4)	Sb9	S13	2.464(4)		S5	2.600(5)
	S23	2.774(5)		S22	2.408(5)		S14	2.966(5)
				S12	2.510(5)		S19	2.721(5)
				S15	2.510(5)		S22	2.556(5)
				S19	2.425(5)			

In parenthesis the standard uncertainty.

ture. All OD structures (polytypes whose layer pairs are geometrically equivalent) obtained by stacking a given layer according to common principle are said to belong to the same family. The operations relating successive layers in general operate in a subspace of the whole crystal space and are thus local symmetry operations. They do not form a group, but a more general algebraic category known as a space groupoid (Brandt, 1927; see also Sadanaga et al., 1980)²⁾. When all the local operations are completed to a global operation, a fictitious structure, common to all OD structures of the same family, is obtained, which is called the family structure (Dornberger-Schiff, 1964).

Homologous series too can often be related to a fundamental structure with smaller unit cell and higher symmetry, which is usually a structure with a close packing topology like galena, halite or nickeline. Hellner (1958) proposed a structural scheme for sulphides in which some minerals are directly related to close packed structures (categories I to III, depending on the occupancies of the

octahedral and tetrahedral holes); others (category IV) have only part of their structure related to a close packed topology; finally, category V included minerals which escape to this classification. The andorite series belongs to category IV and, according to Hellner (1958), the minerals in this series are made up by a distorted galena structure for about 85%. The aristotype for this series is thus certainly less symmetric than a close packed sulphide like galena. Furthermore, differently from polytypes, which can all be obtained by a common aristotype (the family structure) because of the nature of the stacking operation, in a series like the andorite we may expect some differences between the model obtained from the aristotype and the real structure of the mineral. This is equivalent to say that going up from the known structures to the unknown aristotype, we may expect some differences in the latter depending on the starting structure.

Hellner (1958) reported a drawing of the structures of ramdohrite and fizélyite from unpublished results, in a space group of type *Bbmm*. Organova et al. (1982) reported about a synthetic sample called 'andorite-24' having $n = 24$ and possibly corresponding to (now discredited) nakaséite. However, they studied only the subcell corresponding to $n = 1$ (i.e., by taking into account only one

²⁾ In the literature, an alternative definition of "groupoid" was introduced by Hausmann and Ore (1937), namely a set on which binary operations act but neither the identity nor the inversion are included. It is nowadays called a magma.

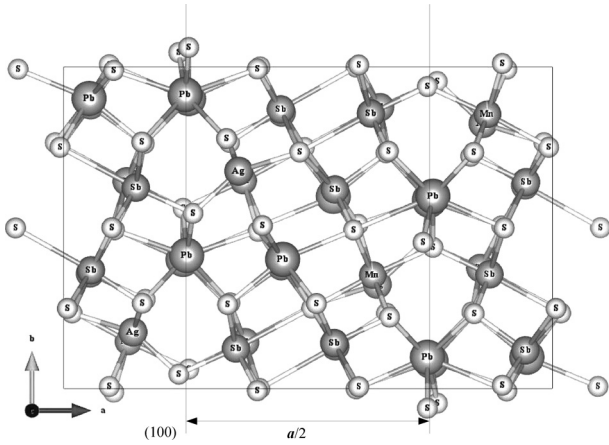


Figure 1. Structure of uchucchacuaite seen in projection along the c axis, where cell-twinning on (100) is seen every $a/2$.

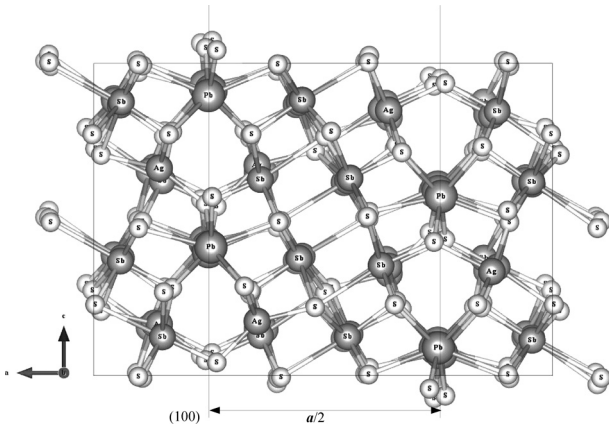


Figure 2. Structure of quatrandorite seen in projection along the b axis, where cell-twinning on (100) is seen every $a/2$ like in uchucchacuaite.

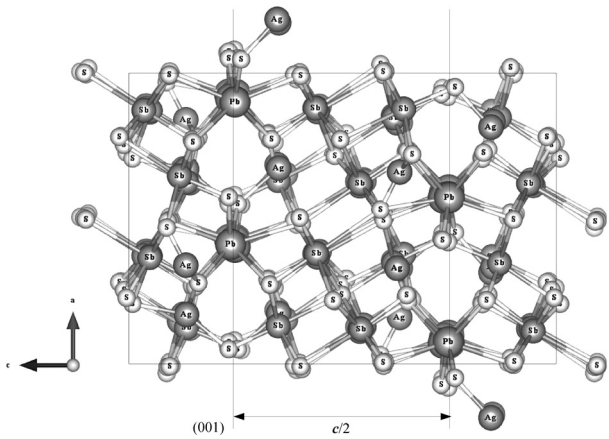


Figure 3. Structure of senandorite seen in projection along the b axis, where cell-twinning on (001) is seen every $c/2$, like in uchucchacuaite and quatrandorite. The difference in indexing comes from the different orientation of the axes in the standard setting of the space group.

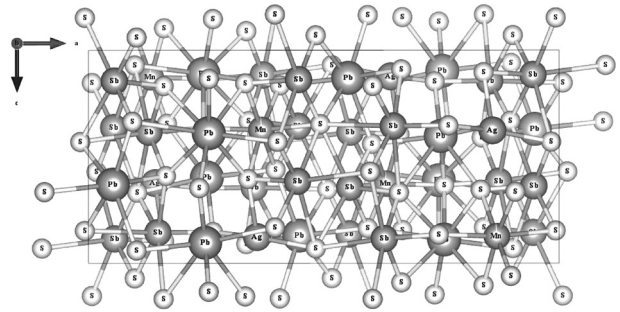


Figure 4. Structure of uchucchacuaite seen in projection along the b axis. The vertical axis c corresponds to $n = 2$.

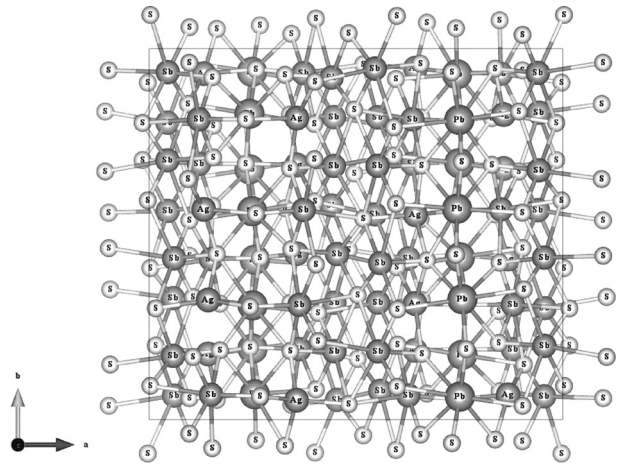


Figure 5. Structure of quatrandorite seen in projection along the c axis. The vertical axis b corresponds to $n = 4$.

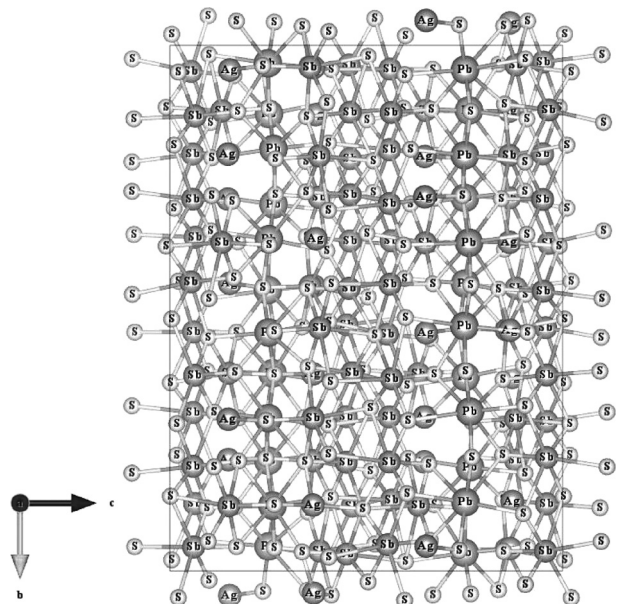


Figure 6. Structure of senandorite seen in projection along the a axis. The vertical axis b corresponds to $n = 6$.

reflection out of 24 along c^*), in a space group of type *Bbmm* like the one previously reported by Hellner. This space-group symmetry is actually an artifact, coming from the widespread twinning in this series (Moëlo et al., 1989). Nevertheless, the possibility of obtaining a reasonable refinement in a subcell with $n = 1$, even if the significance of resulting structure is invalidated by the presence of twinning, has clearly pointed out the importance of the aristotype with of $n = 1$.

With respect to the classical path from aristotype to hettotype, our task is the opposite and definitely more complex. In fact, the hettotypes are known, while a possible aristotype has to be found. The path is thus from group (H , in the following) to supergroup (G , in the following), instead of from group to subgroup, and the number of possibilities is definitely larger. This can however be somehow restricted by the following considerations.

1. The cell parameters of the aristotype have to comply with $n = 1$, i.e., be close to $19/13/4^3$, which means that the aristotype will have an orthorhombic symmetry. There is no need to search for smaller cells because all the known hettotypes have in common two cell parameters, while the third is a multiple of 4.
2. The monoclinic hettotypes are metrically practically orthorhombic; this reduces significantly the number of possible supergroups because practically no cell deformation has to be introduced in the search for aristotypes.

The path from H to G is decomposed in a series of minimal supergroups $H \subset H_1 \subset H_2 \dots \subset G$, i.e., H_i is such a supergroup of H_{i-1} so that there are no intermediate groups between them: H_{i-1} is then called a maximal subgroup of H_i . The first step in the search for a possible aristotype is to locate one or more paths leading to an orthorhombic supergroup with the expected cell parameters. Then, for each path located in the previous step and for each pair H_i and H_{i-1} along this path, the atomic coordinates in H_{i-1} have to be expressed in the setting of H_i , by a transformation that is the inverse of that relating the axial settings of the two groups, because the coordinates transform contravariantly with respect to the basis. The result obtained is not yet compatible with H_i : the atoms have to be moved to match the higher symmetry of H_i . If $O(H)$ is the order of a group H , the ratio $n = O(H_i)/O(H_{i-1})$ is called the index of H_{i-1} in H_i . H_i can be decomposed in terms of H_{i-1} leading to $n-1$ cosets, all with the same length, i.e., containing the same number of elements (symmetry operations in our case), which corresponds to the order of H_{i-1} . Let S be a symmetry element of H_i which does not exist

in H_{i-1} ; a symmetry operation performed about S is a representative of a coset obtained by decomposing H_i in terms of H_{i-1} . The atomic displacement operated to match the additional symmetry in H_i may result in an increase of the site-symmetry group of the position, if the atom moves on S , or in the appearance of equivalence relations between atoms unrelated in H_{i-1} , when the moved atoms become related by S . In the latter case, the number of atoms in the asymmetric unit is reduced, while the site-symmetry group may remain unchanged or be of higher order, if the new position comes to have specialized fractional coordinates. This is the opposite of the Wyckoff position splitting observed when deriving an hettotype from a known aristotype. The largest displacement necessary to match the additional symmetry in H_i with respect to H_{i-1} is a measure of the pseudo-symmetry of the structure in H_i .

The search for aristotypes have been partly performed through the crystallographic tools at the Bilbao Crystallographic Server (Aroyo et al., 2006a, 2006b, 2011); in particular, the group-supergroup paths have been found with the program CELLSUPER, while for the atomic displacements in the supergroups the program PSEUDO (Capillas et al, 2011) has been used. The latter is however more suited to find real pseudo-symmetries and does not necessarily provide the best solution for larger tolerances like those necessary for atomic displacements considered here (M.I. Aroyo, personal communication to MN). For this reason, the additional symmetries of displaced atomic position in the supergroups have been systematically derived also by an ad-hoc software developed on purpose and cross-checked with the results of PSEUDO. A different description may finally be necessary to compare the aristotypes obtained from the different members of the series. Indeed, a structure can be described in a number of different but equivalent ways, through a change of the origin and / or of orientation: the number of equivalent descriptions corresponds to the index of the space group in its Euclidean normalizer (Koch et al, 2005).

Figures 7 to 9 show, respectively, the possible space-group paths from $P2_1/n$ (ramdohrite), $P2_1/c$ (quatrondorite) and $Pna2_1$ (senandorite). The first two obviously correspond to the same type of space group, with a different cell choice: this different choice is of paramount importance to show the practically orthorhombic metric symmetry of the lattice. The end point of a path is always a space-group type with cell parameters $19/13/4$ or any permutation of these. A cross (\times) indicates a dead-end, namely a path not leading to a space-group type with these parameters. Senandorite crystallizes in a pyroelectric type of space group, where the origin is not fixed a

³⁾ For the sake of simplicity, only the integer part is retained below, but all the computations are made with the real cell parameters

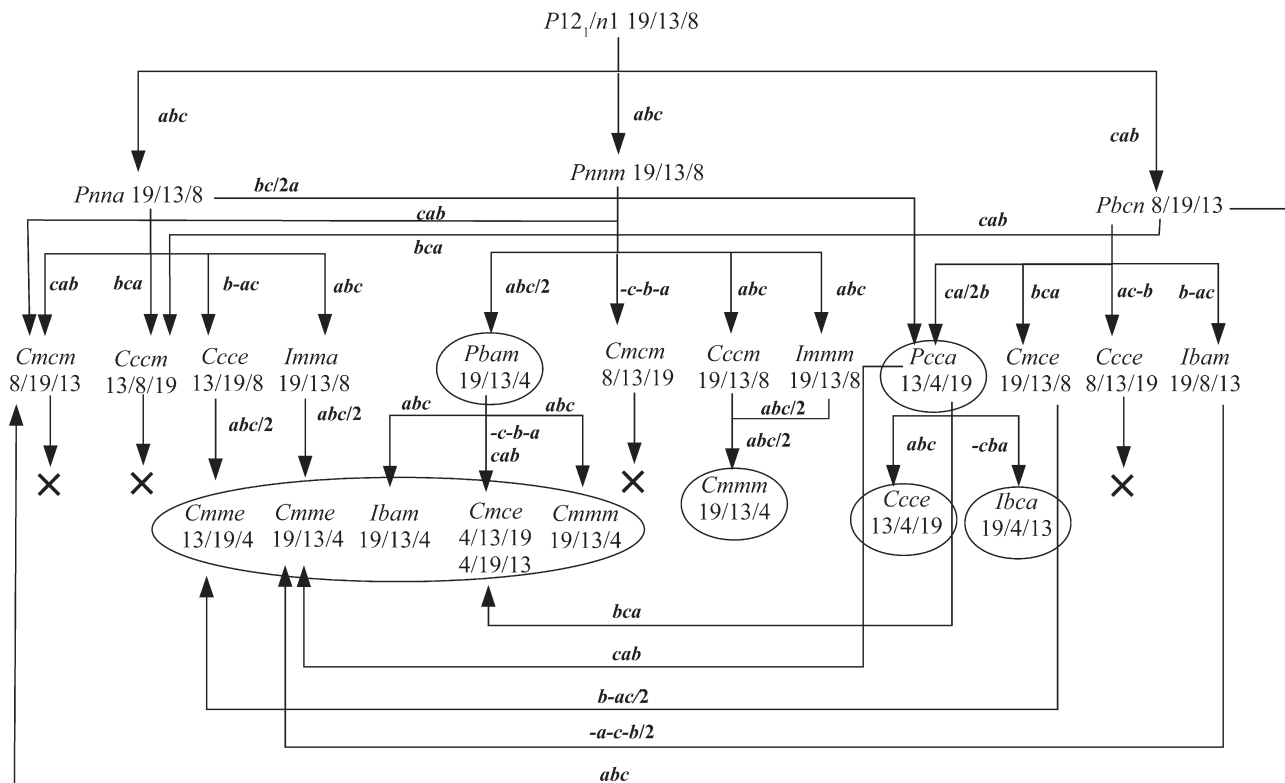


Figure 7. Possible paths from $P2_1/n$ 19/13/8, setting of uchucchacuaite, to all orthorhombic holohedral supergroups corresponding to 19/13/4 or a permutation of these parameters (circled). A cross (X) indicates a dead-end, namely a path not leading to a space-group type with the required parameters. The changes of axial setting is indicated, while the shift of the origin is omitted; the latter is explicitly given in the modified Bärnighausen trees (Figures 10, 11, 13, 14 and 15).

priori: we chose as first step a centro-symmetric supergroup to immediately remove this ambiguity but also because, as discussed below, the degree of pseudo-symmetry in the holohedral supergroup is a measure of the probability of occurrence of twinning.

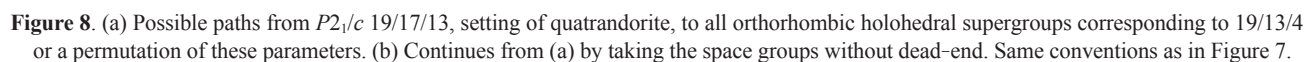
A possible common aristotype for these three structures must have the same type of space group and the cell parameters in the same order. Inspection of the figures shows that only two common supergroups exist, both of type *Cmme*, with cell parameters 19/13/4 or 13/19/4. These are however easily inter-converted by an exchange of the *a* and *b* axes and a shift of the origin (matrix transformation read by rows 010/ $\bar{1}$ 00/001, origin shift $\frac{1}{4}\frac{1}{4}0$), so that a unique candidate is immediately found. As discussed below in details, some atomic displacements along this path are relatively important (larger than 1 Å), which means that to reach the common aristotype a non-negligible local deformation is necessary.

If only smaller atomic displacements are allowed, a different route can be followed for quatrandorite and senandorite, but not for the $n = 2$ minerals, leading to *Cmcm* with the same cell parameters. In the following, we analyze both routes, starting from the second one because of the smaller deformations it requires.

Cmcm aristotype

The paths to *Cmcm* are shown in Figures 10 to 11 by the corresponding modified Bärnighausen trees (Bärnighausen, 1980; for a recent review, see Nespolo, 2008). Each node of a Bärnighausen tree consists of a rectangle containing the label of the atom occupying the atomic position (one taken as representative if the site is statistically occupied by more than one), the Wyckoff letter, the site-symmetry group and the fractional coordinates; the branches are arrows relating the atomic positions. In the left part, the path relating the space groups is shown, where the arrows relate pairs of groups, labeled by the type of subgroup (t, k, i)⁴⁾, the order of the subgroup, followed by the basis vectors of the subgroup in terms of those of the supergroup and by the origin shift. Because

⁴⁾ *t* stands for *translationengleiche* subgroup (common translational lattice, lower geometric crystal class). *k* stands for *klassengleiche* subgroup (common geometric crystal class, less translational symmetry). *i* stands for *isomorphic* space group, a special case of *klassengleiche* where the subgroup is of the same type (same Hermann-Mauguin symbol) as its supergroup.



online from <http://japanlinkcenter.org/DN/JST.JSTAGE/jmps/120730> as deposited material). On the other hand, above each node we have placed the atomic displacement

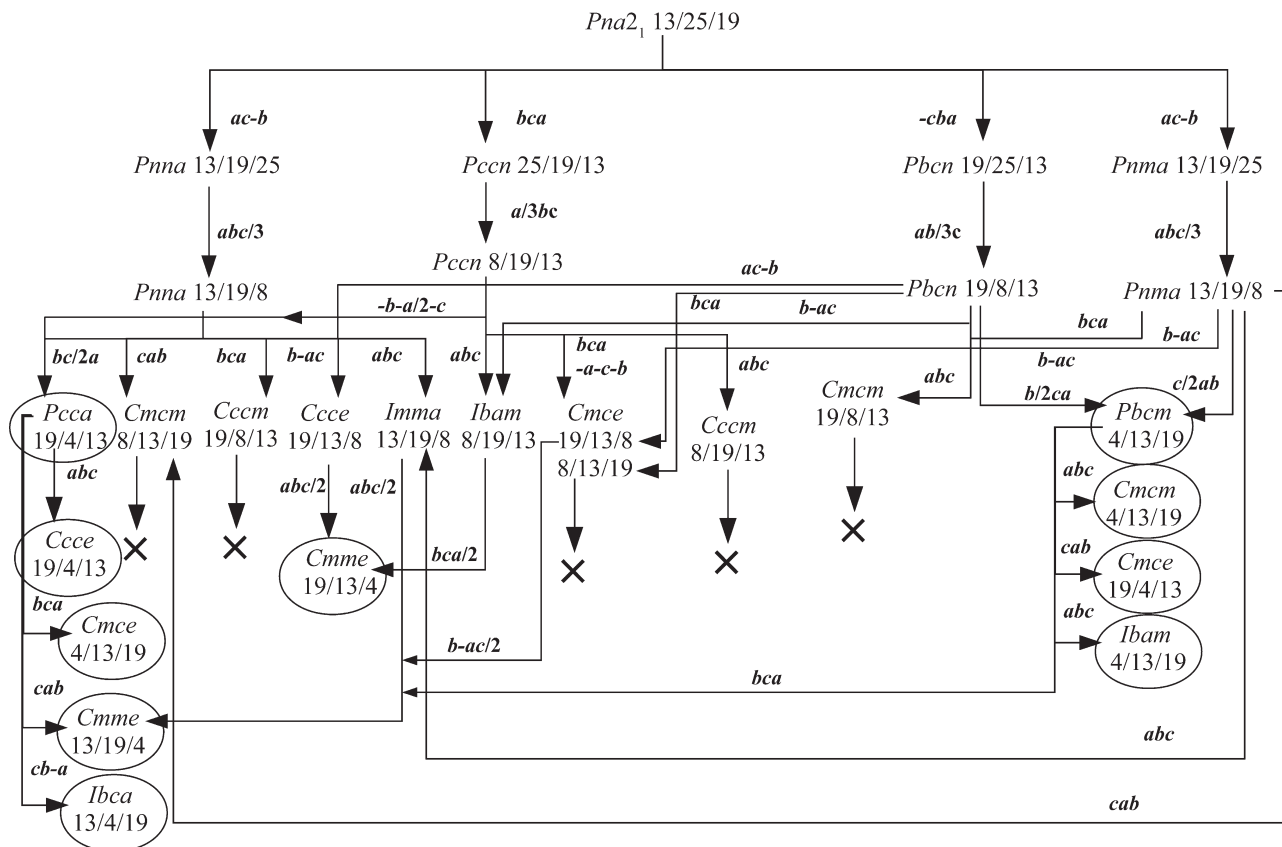


Figure 9. Possible paths from $Pna2_1$ 13/25/19, setting of senandorite, to all orthorhombic holohedral supergroups corresponding to 19/13/4 or a permutation of these parameters. Same conventions as in Figure 7.

needed to place the atom on S , as defined above, or to make pairs of atoms related by S . Bärnighausen trees present the structural path from group to subgroup, while we are exploring the opposite path: Figures 10 and 11 have thus to be read bottom-up. This explains the apparently strange sequence of atomic labels, which comes from the pairing of atoms by pseudo-symmetry S .

Quatrandorite has a very high degree of pseudo-orthorhombic symmetry in *each* of the minimal supergroups up to $Cmcm$: the largest displacement in each step is only 0.58 Å, 0.43 Å, 0.03 Å and 0.08 Å for $P2_1/c$ (19/17/13) \rightarrow $Pbca$ (13/19/17) \rightarrow $Pbcm$ (8/13/19) \rightarrow $Pbcm$ (4/13/19) \rightarrow $Cmcm$ (4/13/19) respectively. The same holds for senandorite, with largest displacements 0.59 Å, 0.08 Å, 0.37 Å and 0.12 Å for $Pna2_1$ (19/25/13) \rightarrow $Pbcn$ (19/25/13) \rightarrow $Pbcn$ (19/8/13) \rightarrow $Pbcm$ (4/13/19) \rightarrow $Cmcm$ (4/13/19) respectively. A difference with respect to the quatrandorite is the presence of an isomorphic group-subgroup relation of index 3 (the b parameter is divided by three): in this step, triples of atoms become equivalent in the supergroup and the corresponding average displacement is indicated; individual displacement are however very close to the average. The fractional coordinates in the aristotype for the two minerals is shown in Table 5, after a change of the or-

igin for senandorite, corresponding to a shift of $a/2 + c/2$, which leads to an equivalent description of the structure. In fact, the Euclidean normalizer of $Cmcm$ is $Pmmm$ ($a/2$, $b/2$, $c/2$), meaning that there are four equivalent descriptions of the same structure in this type of space group, among which the one we have chosen to show the correspondences between the coordinates in the aristotypes obtained from the two minerals. This correspondence in $Cmcm$ is practically perfect. The aristotype is shown in Figure 12.

As shown in Figures 7 to 9, $Cmcm$ is not a possible supergroup for the $n = 2$ member, which does not show a comparable pseudo-symmetry either: in fact, no orthorhombic structure can be obtained by atomic displacement up to 1 Å. To find a common aristotype for the three members of the series, larger atomic displacements have to be allowed.

***Cmme* aristotype**

As discussed above, a path to a common supergroup exists for the three minerals of the series, towards $Cmme$, although the degree of pseudosymmetry for quatrandorite and senandorite along this path is lower.

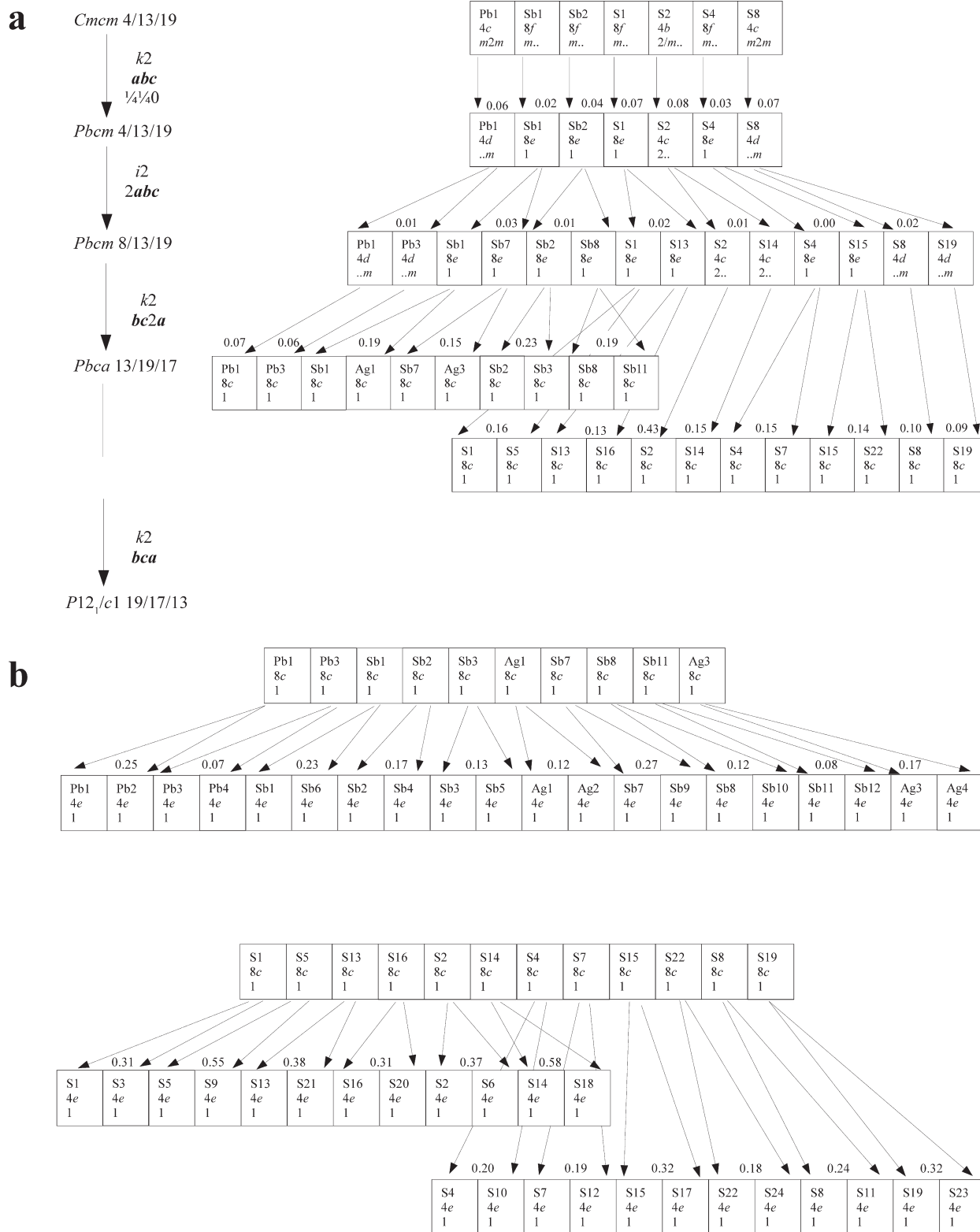


Figure 10. (a) Modified Bärnighausen tree for quatrondorite towards *Cmcm* 4/13/19. The fractional numbers above each node indicate the atomic displacement needed to move atoms from the positions of a subgroup to those of the supergroup. The tree has been constructed bottom-up, from the known hettotype to the unknown aristotype. The small atomic displacements show the high degree of pseudosymmetry of the structure. (b) shows the splitting of positions in the last group-subgroup pair.

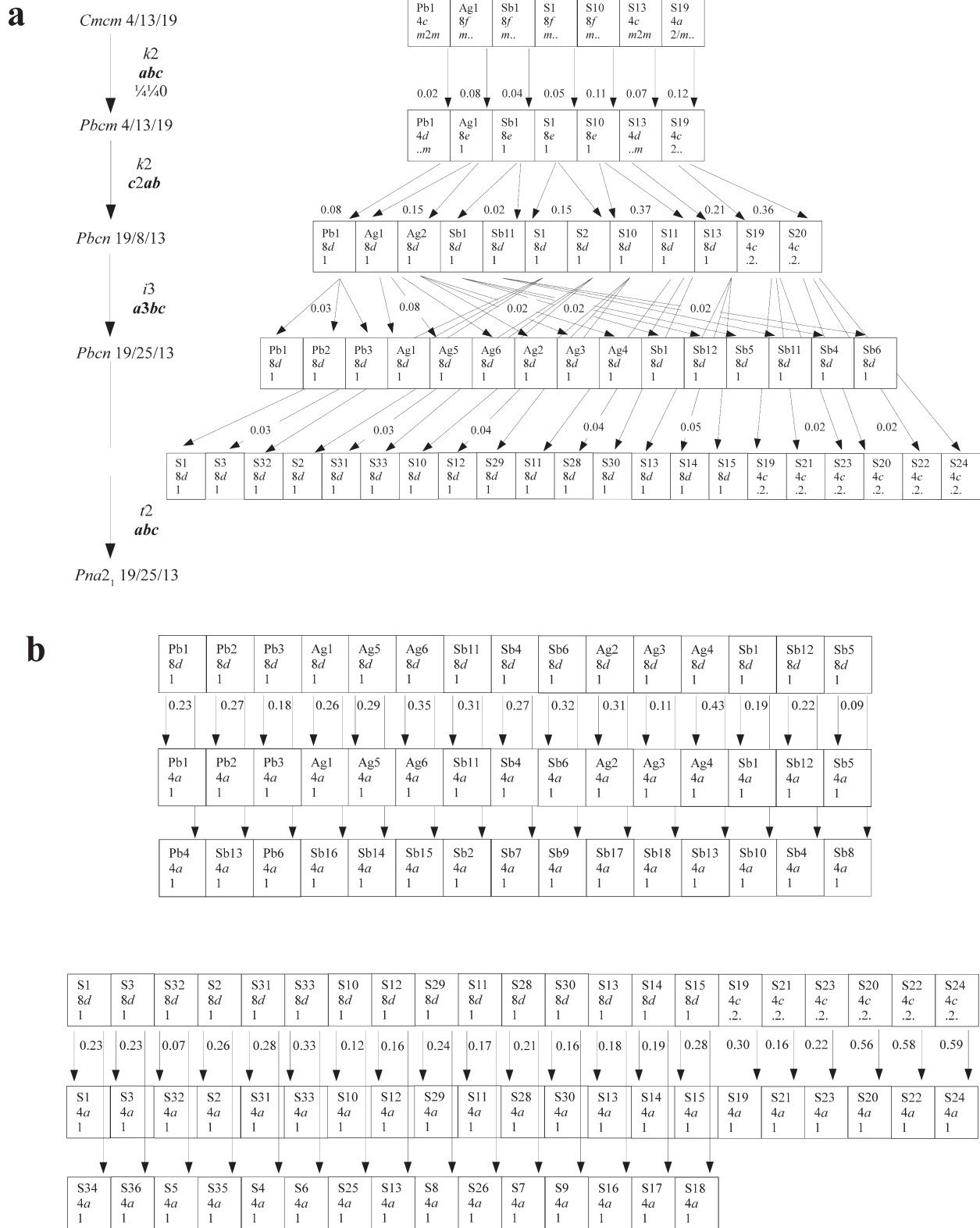


Figure 11. Modified Bärnighausen tree for senandorite towards *Cmcm* 4/13/19. Same conventions as in Figure 10. The small atomic displacements show the high degree of pseudosymmetry of the structure.

Table 5. Fractional coordinates in the aristotype *Cmcm* 4/13/19 for quatranderite and senanderite *

Quatranderite					Senanderite			
Label	Position	<i>x</i>	<i>y</i>	<i>z</i>	Position	<i>x</i>	<i>y</i>	<i>z</i>
M1	4 <i>c</i>	0.5	0.83844	0.25	4 <i>c</i>	0.5	0.83397	0.25
M2	8 <i>f</i>	0	0.59903	0.13686	8 <i>f</i>	0	0.59757	0.13658
M3	8 <i>f</i>	0.5	0.62622	0.94782	8 <i>f</i>	0.5	0.62740	0.94823
S1	8 <i>f</i>	0	0.25885	0.40213	8 <i>f</i>	0	0.25858	0.40134
S2	4 <i>b</i>	0	0.5	0	4 <i>b</i>	0	0.5	0
S3	8 <i>f</i>	0.5	0.47570	0.16100	8 <i>f</i>	0.5	0.47458	0.16066
S4	4 <i>c</i>	0	0.69293	0.25	4 <i>c</i>	0	0.68733	0.25

* No such aristotype can exist for uchucchacuaite: see Figure 7 and text.

The first three positions correspond to cations, the other four to sulfur atoms.

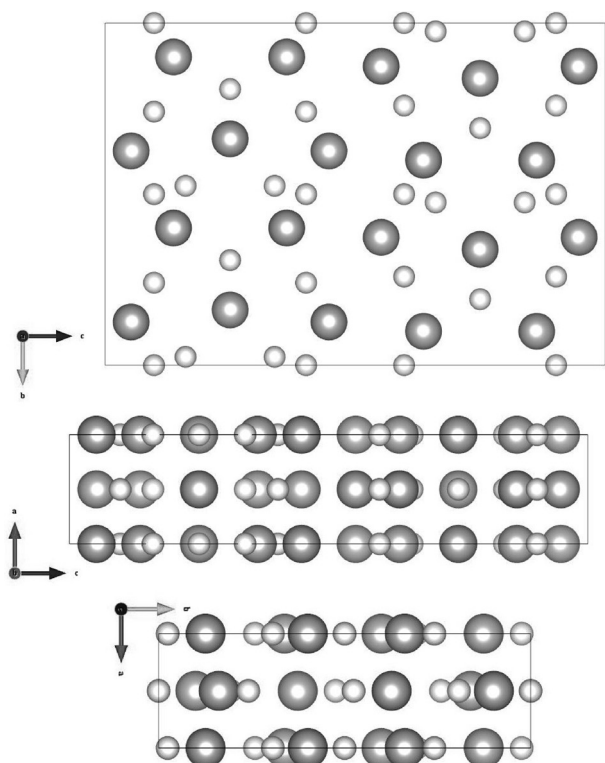


Figure 12. The aristotype *Cmcm* 4/13/19 common to quatranderite and senanderite, seen in projection along *a* (top), *b* (middle) and *c* (bottom). Gray, cations; white, anions.

Ramdohrite, fizélyite and uchucchacuaite all correspond to $n = 2$ and are thus essentially isostructural; in uchucchacuaite part of the silver is substituted by manganese. The refinement of the ramdohrite structure reported by Makovicky and Mumme (1983) was of low quality ($R = 19.3\%$) and the new refinement from the same sample is still unpublished. In the Ag-rich fizélyite reported by Yang et al. (2009), two cation sites are split and an additional silver site occurs, which is unoccupied in ramdohrite. The uchucchacuaite structure reported by Yang et al. (2011), refined up to $R = 3.7\%$ and 3.1% on two different samples, is the best candidate.

The path followed in the search for aristotype is $P2_1/n - Pnna - Imma - Cmme$ (Figure 13). This path allows to keep the axes parallel to each other; an origin shift of $\frac{1}{4}\frac{1}{4}\frac{1}{4}$ is necessary in going from *Pnna* to *Imma*; in the last step, the *c* axis is halved, which means that the *z* coordinate of each atom is doubled. The modified Bärnighausen tree in Figure 13 shows the opposite path.

The first step, from $P2_1/n$ to *Pnna*, requires atomic displacements ranging from 0.42 Å (pairing of S7 and S11: the site-symmetry group of the new position is unchanged but the multiplicity is doubled) to 1.59 Å (S8 moving from general to special position). Ten atoms are promoted from general position in $P2_1/n$ to special position in *Pnna* (Pb1, Pb2, S2, S3, S4, S6, S8, S9, S10, S12), while the other twelve atoms stay in general position also in the supergroup but become pairwise related by the additional symmetry operations *S*. The interpretation of the next steps is straightforward.

Figure 14 shows the same derivation for quatranderite. With respect to Figure 10, the path diverges after *Pbca* and the pseudosymmetry is lower (larger atomic displacements).

Figure 15 is for senanderite. Here again, with respect to Figure 11, the path diverges after *Pbcn* and the pseudosymmetry is lower.

The final result, i.e., the atomic coordinates in the aristotype, are given in Table 6; the first two rows correspond to cations (indicated as M1, M2), the other four to sulfur atoms (relabelled as S1 to S4). As for *Cmcm*, a different choice of the origin has been taken, in this case for the aristotype obtained from quatranderite, corresponding to a shift of $c/2$: the Euclidean normalizer of *Cmme* is again *Pmmm* ($a/2$, $b/2$, $c/2$). Inspection of the table, as well as of Figure 16, where the aristotypes are drawn in projection along the *b* axis, shows that the bulk of the three structures perfectly matches in the *Cmme* aristotype, while the position of a sulfur atom differs. In fact, the second sulfur goes in position 4*a* from uchucchacuaite and quatranderite, but to position 4*b* from senanderite; the

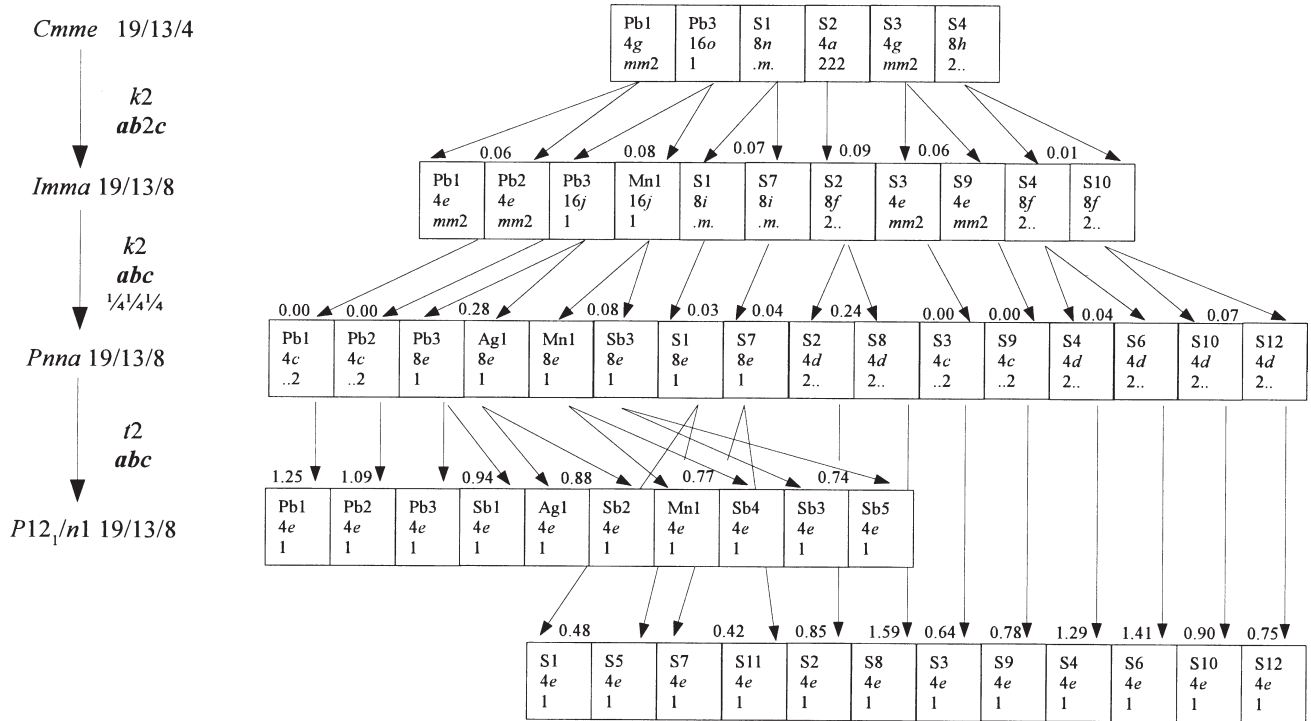
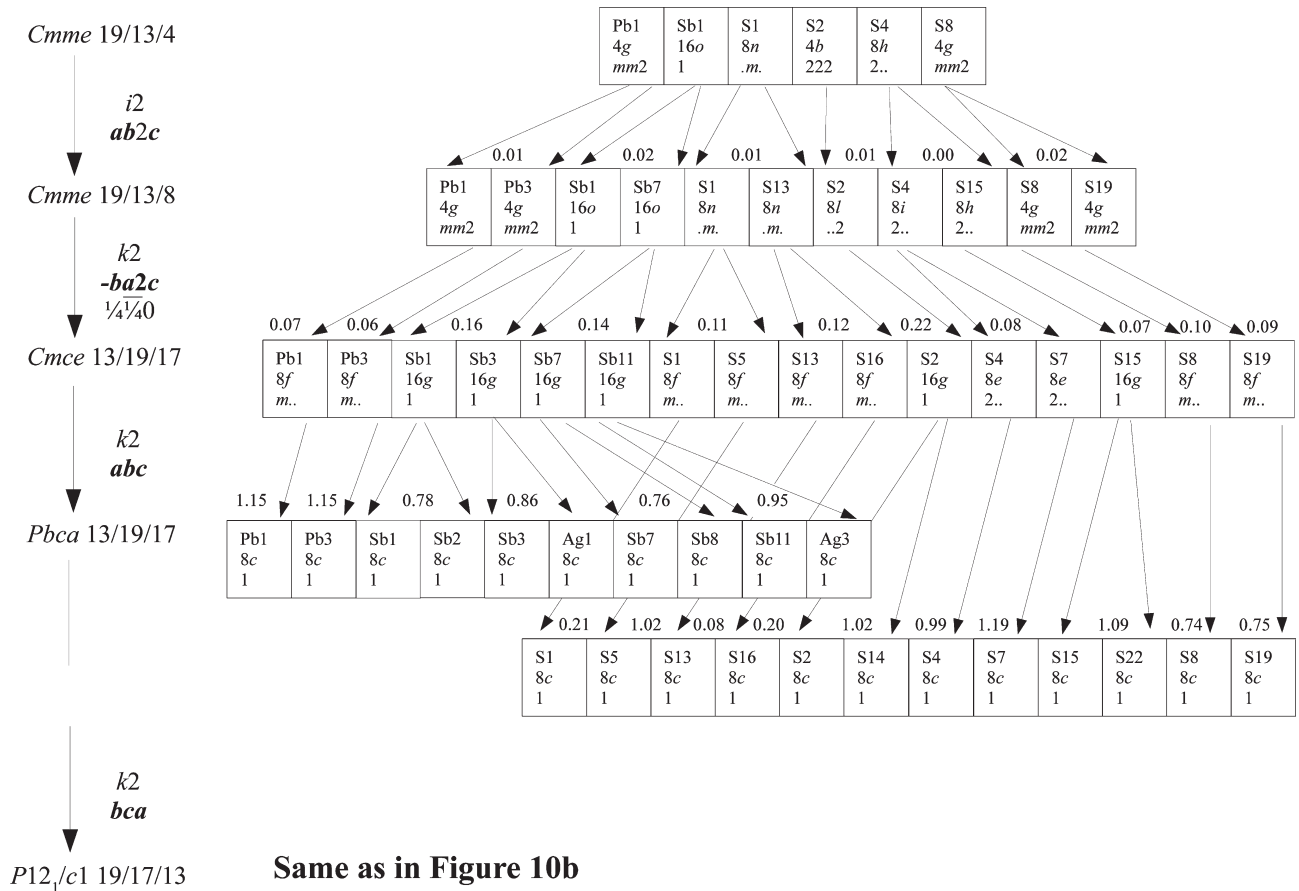
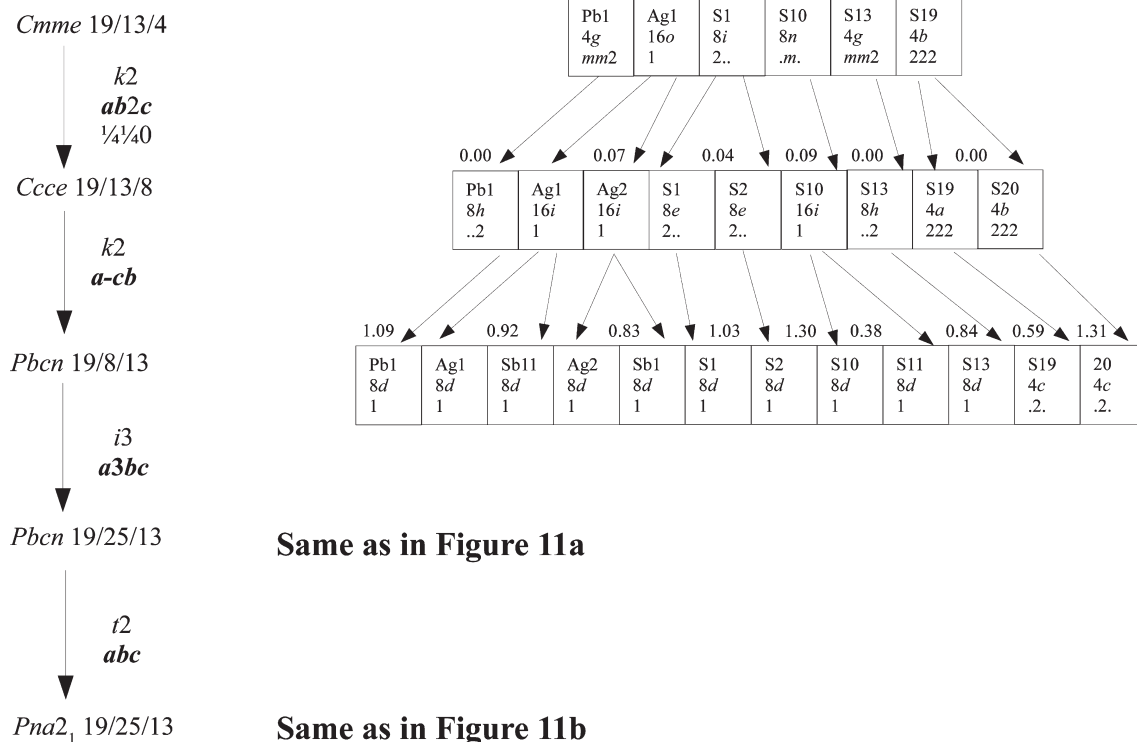


Figure 13. Modified Bärnighausen tree for uchucchacuaite. Same conventions as in Figure 10.

Figures 14. Modified Bärnighausen tree for quatrondorite towards *Cmme*. Same conventions as in Figure 10.



Figures 15. Modified Bärnighausen tree for senandorite towards *Cmme*. Same conventions as in Figure 10.

Table 6. Fractional coordinates in the aristotype *Cmme* 19/13/4 *

Uchucchacuaite					Quatrandorite				Senandorite			
Label	Position	x	y	z	Position	x	y	z	Position	x	y	z
M1	16o	0.84586	0.61458	0.75892	16o	0.84452	0.61263	0.75675	16o	0.84417	0.61249	0.74727
M2	4g	0	0.75	0.29256	4g	0	0.75	0.23592	4g	0	0.75	0.2676
S1	8n	0.1505	0.75	0.26822	8n	0.15213	0.75	0.23320	8n	0.15134	0.75	0.27500
S2	4a	0.75	0.5	0	4a	0.75	0.5	0	4b	0.75	0.5	0.5
S3	4g	0	0.75	0.78051	4g	0	0.75	0.73330	4g	0	0.75	0.76700
S4	8h	0.08700	0.5	0	8i	0.08900	0.5	0.5	8i	0.08933	0.5	0.5

* Obtained from the Bärnighausen trees in Figures 10 to 12.

A difference of $c/2$ exists in *one* position: 8h versus 8i between uchucchacuaite and quatrandorite, and 4a versus 4b between uchucchacuaite and senandorite.

fourth sulfur goes to position 8h from uchucchacuaite but to position 8i from quatrandorite and senandorite. Positions 4a and 4b on one side, and 8h and 8i on the other side, differ by $c/2$ and belong to the same Wyckoff set, i.e., they are equivalent in the Euclidean normalizer; in other words, the structures in *Cmme* obtained from the three minerals are conjugated in the Euclidean normalizer. This well agrees with Hellner's analysis, according to which the bulk of the structure of the minerals of the andorite series is made up of a distorted galena. The remaining difference is however crucial to obtain the real structures of the three minerals from the common aristotype.

STRUCTURAL PSEUDOSYMMETRY AND THE PERVASIVE TWINNING IN THE ANDORITE SERIES

Minerals in the andorite series are almost invariably twinned. The reticular theory of twinning, developed by the 'French school' and summarized in the classical textbook by Friedel (1926), gives the necessary conditions for twinning in terms of the degree of lattice restoration produced by the twin operation. The members corresponding to $n = 2$ and $n = 4$ are monoclinic holohedral but metrically practically orthorhombic: twinning in the orthorhombic holohedry gives thus a perfect lattice restoration, which is a strong condition for twinning. Senandorite, on the other

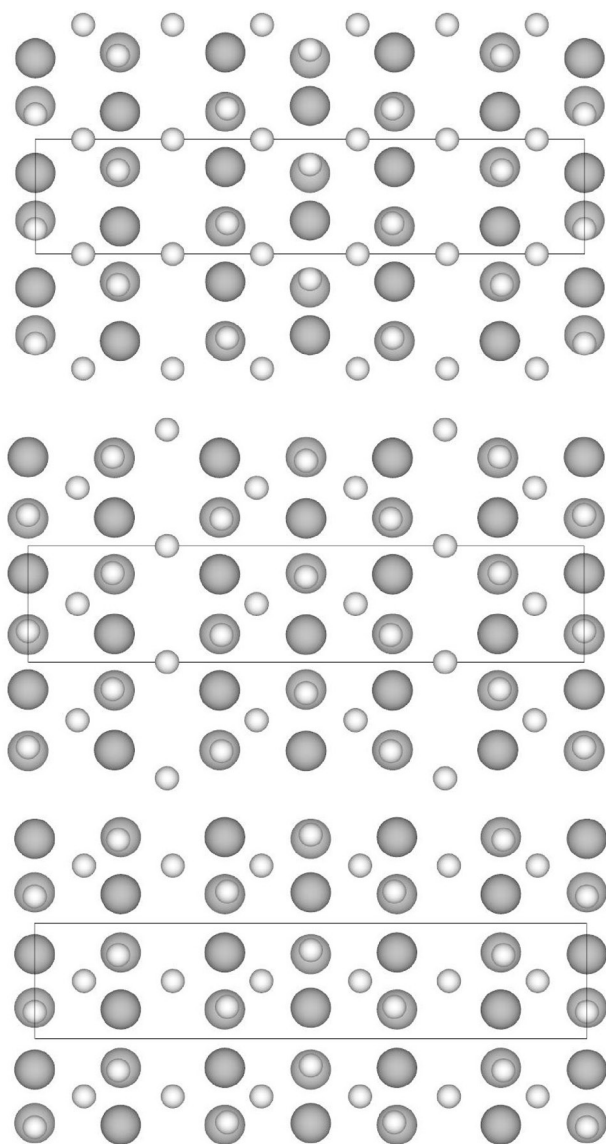


Figure 16. The *Cmme* aristotype of uchucchacuaite (top), quatrandorite (middle) and senandorite (bottom), in projection along the *b* axis. Gray, cations; white, anions.

hand, is orthorhombic hemihedral and inversion twinning can be easily predicted.

Lattice restoration is a necessary, but not sufficient condition for twinning; sufficient conditions have to be found in the structural match, in particular across the twin interface. When the whole structure continues unperturbed across the interface, one gets a single crystal (or a parallel growth), not a twin. When part of the structure continues, more or less unperturbed, while the rest loses continuity at the interface, a twin is formed if the substructure crossing the interface is large enough to ensure the stability of the crystalline edifice (Nespolo and Ferraris, 2009).

The search for the sufficient conditions for twinning

in terms of substructure continuity at the interface in the general case is a complex task requiring consideration of the eigensymmetry of non-characteristic crystallographic orbits and of the layer groups corresponding to the thin region at the interface common to the individuals. In the case twinning by merohedry, however, when the lattice restoration is complete, an easier, although less general, approach is to evaluate the degree of structural pseudosymmetry in a supergroup belonging to the holohedry of the twin lattice. For the minerals of the andorite series, this supergroup is the orthorhombic holohedral supergroup which makes the first step in the search for aristotype analyzed above.

For uchucchacuaite, five atoms move by 1 Å or more (the largest displacement is 1.59 Å) in the *Pnna* supergroup. The two other orthorhombic supergroups do not lead to the *Cmme* aristotype; furthermore, the pseudosymmetry is less pronounced: in *Pnnm* ten atoms move by 1 Å or more, although the largest displacement is a bit smaller (1.47 Å); in *Pbcn* the situation is definitely worse, S6 having to move by more than 2 Å. The structural pseudo-orthorhombic symmetry in uchucchacuaite is therefore imperfect and concerns only part of the structure.

For quatrandorite and senandorite, the pseudo-symmetry is extensive for the whole structure, not only in the orthorhombic minimal supergroup but up to *Cmcm* 4/13/19, which makes the occurrence of twinning a high probability event and explains why twinning in quatrandorite is “ubiquitous”, as stated by Moëlo et al. (1989). The fact the our sample was not twinned must therefore be considered a rather exceptional event.

DISCUSSION

The structure of quatrandorite, reported here for the first time, completes the picture of the andorite series, dominated by the strong pseudo-symmetry which concerns part of the structure for the $n = 2$ member but the whole structure for the $n = 4$ and $n = 6$ members. This marked pseudo-symmetry explains the pervasive twinning in the minerals of the series.

The strong pseudo-symmetry of the whole structure of both quatrandorite and senandorite leads, through minimal atomic displacement, to a common aristotype (*Cmcm*) for these two members, which is not shared by the $n = 2$ member. To find a common aristotype for all the three members (*Cmme*), larger atomic displacements have to be allowed, which means a path with lower pseudo-symmetry; furthermore, despite this larger deformation, a difference in the position of a sulfur atom remains in the aristotypes obtained from the three members.

These results suggest a fundamental difference be-

tween the $n = 2$ and the other members; the coexistence of quatrandorite and senandorite as a random stacking, which has been in the past erroneously interpreted as a new mineral ('nakaséite'), points in the same direction. To our knowledge, no such coexistence has been reported for the $n = 2$ member. Whether this structural difference between the latter and the other members of the series comes from a difference in composition or in the conditions for formation is not known but certainly deserves further studies.

ACKNOWLEDGMENTS

This research has been performed during a stay of MN as invited Professor at the Institute of Materials Research, Tohoku University. MN thanks Prof. Mois I. Aroyo (Universidad del Pays Vasco, Bilbao) and Prof. Vaclav Petricek (Academy of Sciences of the Czech Republic) for useful discussions, and Dr. Valery Chani (IMR, Tohoku University) for help with the Russian literature. The critical remarks by Prof. Takeo Matsumoto (Kanazawa University) and an anonymous referee are gratefully acknowledged.

SUPPLEMENTAL MATERIALS

Details of the aristotypes derivation as well as the CIF (Crystallographic Information File) for quatrandorite are available online from <http://japanlinkcenter.org/DN/JST.JSTAGE/jmps/120730>.

REFERENCES

- Aroyo, M.I., Perez-Mato, J.M., Capillas, C., Kroumova, E., Ivantchev, S., Madariaga, G., Kirov, A. and Wondratschek, H. (2006a) Bilbao Crystallographic Server I: Databases and crystallographic computing programs. *Zeitschrift für Kristallographie*, 221, 15–27.
- Aroyo, M.I., Kirov, A., Capillas, C., Perez-Mato, J.M. and Wondratschek, H. (2006b) Bilbao Crystallographic Server II: Representations of crystallographic point groups and space groups. *Acta Crystallographica*, A62, 115–128.
- Aroyo, M.I., Perez-Mato, J.M., Orobengoa, D., Tasci, E.S., de la Flor, G. and Kirov, A. (2011) Crystallography online: Bilbao Crystallographic Server. *Bulgarian Chemical Communications*, 43, 183–197.
- Bärnighausen, H. (1980) Group-subgroup relations between space groups: a useful tool in crystal chemistry. *MATCH, Communications in Mathematical Chemistry*, 9, 139–175.
- Belsky, A., Hellenbrandt, M., Karen, V.L. and Luksch, P. (2002) New developments in the Inorganic Crystal Structure Database (ICSD): accessibility in support of materials research and design. *Acta Crystallographica*, B58, 364–369.
- Brandt, H. (1927) Über eine Verallgemeinerung des Gruppenbegriffes. *Mathematische Annalen*, 96, 360–366.
- Buerger, M.J. (1947) Derivative structures. *Journal of Chemical Physics*, 15, 1–16.
- Capillas, C., Tasci, E.S., de la Flor, G., Orobengoa, D., Perez-Mato, J.M. and Aroyo, M.I. (2011) A new computer tool at the Bilbao Crystallographic Server to detect and characterize pseudosymmetry. *Zeitschrift für Kristallographie*, 226, 186–196.
- Dornberger-Schiff, K. (1956) On Order-Disorder Structures (OD-Structures). *Acta Crystallographica*, 9, 593–601.
- Dornberger-Schiff, K. (1964) Grundzüge einer Theorie von OD-Strukturen aus Schichten. *Abhandlungen der Deutschen Akademie der Wissenschaften, Klasse für Chemie, Geologie und Biologie*, 3, 107.
- Friedel, G. (1926) *Leçons de Cristallographie*. Berger-Levrault, Nancy, Paris, Strasbourg, pp. XIX+602.
- Hausmann, B.A. and Ore, O. (1937) Theory of quasigroups. *American Journal of Mathematics*, 59, 983–1004.
- Hellner, E. (1958) A structural scheme for sulfide minerals. *Journal of Geology*, 66, 503–525.
- Ito, T. and Muraokawa, H. (1960) Nakaséite, an andorite-like new mineral. *Zeitschrift für Kristallographie*, 113, 94–98.
- Koch, E., Fischer, W. and Müller, U. (2005) Normalizers of Space Group. Chapter 15 in *International Tables for Crystallography Vol. A, Space Group Symmetry*, 5th revised edition (Hahn, Th. Edit.). Dordrecht, Boston, London: Kluwer Academic Publishers.
- Makovicky, E. and Mumme, W.G. (1983) The crystal structure of ramdohrite, $\text{Pb}_6\text{Sb}_{11}\text{Ag}_3\text{S}_{24}$, and its implications for the andorite group and zinckenite. *Neues Jahrbuch für Mineralogie. Abhandlungen*, 147, 58–79.
- Megaw, H.D. (1973) *Crystal Structures: a Working Approach*. Philadelphia: Saunders Co.
- Moëlo, Y., Makovicky, E. and Karup-Møller, S. (1989) Sulfures complexes plombo-argentifères : minéralogie et cristallographie de la série andorite-fizélyite, $(\text{Pb}, \text{Mn}, \text{Fe}, \text{Cd}, \text{Sn})_{3-2x}(\text{Ag}, \text{Cu})_x(\text{Sb}, \text{Bi}, \text{As})_{2+x}(\text{S}, \text{Se})_6$. *Documents du BRGM*, 167. Éditions du BRGM, Orléans.
- Momma, K. and Izumi, F. (2008) VESTA: a three-dimensional visualization system for electronic and structural analysis. *Journal of Applied Crystallography*, 41, 653–658.
- Nespolo, M. (2008) Does mathematical crystallography still have a role in the XXI century? *Acta Crystallographica*, A64, 96–111.
- Nespolo, M. and Ferraris, G. (2000) Twinning by syngonic and metric merohedry. Analysis, classification and effects on the diffraction pattern. *Zeitschrift für Kristallographie*, 215, 77–81.
- Nespolo, M., Ferraris, G., Đurovič, S. and Takéuchi, Y. (2004) Twins vs. modular crystal structures. *Zeitschrift für Kristallographie*, 219, 773–778.
- Nespolo, M. and Ferraris, G. (2009) A survey of hybrid twins in non-silicate minerals. *European Journal of Mineralogy*, 21, 673–690.
- North, A.C.T., Phillips, D.C. and Matheus, F.S. (1968) A semi-empirical method of absorption correction. *Acta Crystallographica*, A24, 351–359.
- Organova, N.I., Kuzmina, O.V., Bortnikov, N.S. and Mozgova, N.N. (1982) Crystal structure of the subcell of synthetic andorite-24. *Doklady Akademii Nauk SSSR*, 267, 939–942.
- Petricek, V., Dusek, M. and Palatinus, L. (2006) Jana2006. The crystallographic computing system. Institute of Physics, Praha, Czech Republic.
- Sadanaga, R., Sawada, T., Ohsumi, K. and Kamiya, K. (1980) Classification of superstructures by symmetry. *Journal of the*

- Japanese Association of Mineralogists, Petrologist and Economic Geologists, Special Issue No. 2: 23–29.
- Sawada, H., Kawada, I., Hellnwr, E. and Tokonami, M. (1987) The crystal structure of senandorite (andorite-VI): PbAgS_3S_6 . *Zeitschrift für Kristallographie*, 180, 141–150.
- Takéuchi, Y. (1997) Tropochemical cell-twinning: A Structure-Building Mechanism in Crystalline Solids. Terra Scientific Publishing Company, Tokyo.
- Wondratschek, H. (1993) Splitting of Wyckoff positions (orbits). *Mineralogy and Petrology*, 48, 87–96.
- Yang, H., Downs, R.T., Burt, J.B. and Costin, G. (2009) Structure refinement of an untwinned single crystal of Ag-excess fizelyite, $\text{Ag}_{5.94}\text{Pb}_{13.74}\text{Sb}_{20.84}\text{S}_{48}$. *Canadian Mineralogist*, 47, 1257–1264.
- Yang, H., Downs, R.T., Evans, S.H., Feinglos, M.N. and Tait, K.T. (2011) Crystal structure of uchucchacuaite, $\text{AgMnPb}_3\text{Sb}_5\text{S}_{12}$, and its relationship with ramdohrite and fizelyite *American Mineralogist*, 96, 1186–1189.

Manuscript received July 30, 2012

Manuscript accepted October 31, 2012

Manuscript handled by Akira Yoshiasa